



Impact of Opportunistic Transmission on MCIK-OFDM: Diversity and Coding Gains

Thien Van Luong and Youngwook Ko^(✉)

Institute of ECIT, Queen's University Belfast, Belfast BT3 9DT, UK
{tluong01,y.ko}@qub.ac.uk

Abstract. This work proposes an opportunistic scheduling scheme for Multi-Carrier Index Keying - Orthogonal Frequency Division Multiplexing (MCIK-OFDM), which is termed as OS-MCIK-OFDM. Particularly, in every transmission, the proposed scheme allows only one machine whose worst sub-channel is the maximum among several machines' worst sub-channels, to communicate with the central device, employing MCIK-OFDM technique. As a result, OS-MCIK-OFDM can harvest the multi-user diversity gain to enhance the reliability of MCIK-OFDM, especially when the number of machines increases. For performance analysis, we derive the closed-form expression for the symbol error probability (SEP), which is then asymptotically analyzed to develop unique features that can address achievable diversity and coding gains, as well as impacts of system parameters. Finally, simulation results are presented to validate the accuracy of the derived SEP performance of OS-MCIK-OFDM and specifically its superiority over the opportunistic scheduling OFDM.

Keywords: MICK-OFDM · OFDM-IM · Index modulation · IM
Opportunistic scheduling · Symbol error probability (SEP)

1 Introduction

Multi-carrier Index Keying - Orthogonal Frequency Division Multiplexing (MCIK-OFDM) or the so-called OFDM with Index Modulation (OFDM-IM) has been recently proposed as an appealing multi-carrier modulation for future wireless communication systems [1, 2]. Unlike the classical OFDM, in every MCIK-OFDM transmission, only a subset of sub-carriers are activated to carry data bits through not only the M -ary modulation symbols, but also the indices of active sub-carriers. This interestingly makes MCIK-OFDM more reliable and energy efficient than the conventional OFDM. In addition, MCIK-OFDM can provide a better trade-off between the reliability and the spectral efficiency (SE), just by changing the number of active sub-carriers.

A wide range of MCIK-OFDM concepts have been proposed to improve either the bit error rate (BER) or the SE performance, which can be found in the survey [3]. For example, in [4, 5], the simple repetition code is proposed to MCIK-OFDM and the resulting scheme called as ReMO can provide the better BER

than more complex IM systems in [6, 7]. A tight bound on the BER is derived in [8], while the achievable rate and the outage probability of MCIK-OFDM are analyzed in [9, 10], respectively. The combinations of MCIK-OFDM with diversity reception techniques and the low-complexity greedy detector are presented in [11, 12]. To increase the SE, in [13], the authors apply the IM concept to both in-phase and quadrature components to double index bits. Besides, a number of methods aiming at boosting the SE can be seen in [14, 15]. The application of MCIK-OFDM to the multi-input multi-output (MIMO) framework is presented in [16]. Recently, impacts of channel state information (CSI) uncertainty on the symbol error probability (SEP) and the BER of MCIK-OFDM are investigated in [17, 18], respectively. In [19], a number of spreading matrices are employed to noticeably increase the diversity gain of MCIK-OFDM.

It is worth mentioning that none of existing works has explored the multi-user diversity improvement in the MCIK-OFDM framework. Thus, in this paper, we study the opportunity of employing the multi-user diversity scheme to enhance the reliability of MCIK-OFDM. More specifically, main contributions of this work are as follows:

- We first propose an opportunistic scheduling MCIK-OFDM (OS-MCIK-OFDM) scheme, in which only one machine with the worst sub-channel being maximum is selected to communicate with the central device, employing MCIK-OFDM technique in every transmission. Such the scheduling strategy can enable the proposed scheme to harvest a notable multi-machine diversity gain when the number of machine increases.
- The average SEP is derived in closed-form, which is then asymptotically analyzed to provide insights into diversity and coding gains achieved by OS-MCIK-OFDM, and effects of system parameters on the SEP performance. We also theoretically compare the average SEPs between the proposed scheme and the opportunistic scheduling OFDM (OS-OFDM) with the same scheduling criterion.
- Simulations results are provided to validate the performance of our proposed scheme and the theoretical analysis. It is shown that OS-MCIK-OFDM significantly outperforms OS-OFDM in terms of the SEP performance.

The rest of the paper is organized as follows. Section 2 introduces the system model. The SEP performance analysis is carried out in Sect. 3. Section 4 presents simulation results, while Sect. 5 concludes the paper.¹

2 System Model

Consider an uplink multicarrier multi-user system where Q machines communicate with a central access point (AP), using the MCIK-OFDM technique. Assume

¹ *Notation:* Upper-case bold and lower-case bold letters represent matrices and vectors, respectively. $(\cdot)^T$, $\|\cdot\|$, $C(\cdot)$ and $\lfloor \cdot \rfloor$ denote the transpose operator and the Frobenious norm, the binomial coefficient and the floor function, respectively. $\mathcal{CN}(0, \sigma^2)$ denotes the complex Gaussian distribution with zero mean and variance σ^2 . $\mathbb{E}\{\cdot\}$ and $\mathcal{M}(\cdot)$ denote the average value and the moment generating function, respectively.

that all machines and the AP are equipped with a single antenna. At each timeslot, only one out of Q machines is opportunistically selected to send its data to the AP, employing MCIK-OFDM with N available sub-carriers.

In particular, denote by $h_q(\alpha)$ the channel from the q -th machine to the AP at sub-carrier α , where $q = 1, \dots, Q$ and $\alpha = 1, \dots, N$. Suppose that $h_q(\alpha)$ represents the Rayleigh fading channels as being independent and identically distributed (i.i.d) complex Gaussian random variable (RVs) with zero mean and unit variance, i.e., $h_q(\alpha) \sim \mathcal{CN}(0, 1)$. Notice from [17] that the error performance of MCIK-OFDM mainly depends on the worst sub-channel, we propose an opportunistic scheduling scheme for MCIK-OFDM, called as OS-MCIK-OFDM, where the AP selects the q^* -th machine to communicate, satisfying

$$q^* = \arg \left\{ \max_{q=1, \dots, Q} \left[\min_{\alpha=1, \dots, N} \left(|h_q(\alpha)|^2 \right) \right] \right\}. \quad (1)$$

Here, the AP is assumed to perfectly know the CSI from all Q machines to conduct such the scheduling strategy. It is noteworthy that by exploiting the multi-machine diversity, OS-MCIK-OFDM is expected to improve the error performance over the classical MCIK-OFDM.

As for the MCIK-OFDM transmission, the selected machine dynamically activates only K out of N sub-carriers to carry data bits via K complex M -ary symbols and indices of active sub-carriers, while the remaining $N - K$ ones are zero padded. Specifically, in every transmission, p incoming data bits are divided into two bit streams ($p = p_1 + p_2$). The first p_1 bits enters an index mapper to identify a combination of K active indices, which is denoted by $\theta = \{\alpha_1, \dots, \alpha_K\}$, where $\alpha_k \in \{1, \dots, N\}$ for $k = 1, \dots, K$. The index set θ can be referred as an index symbol. While, the remaining p_2 bits enters an M -ary mapper to be mapped to K data symbols denoted by $\mathbf{s} = [s(\alpha_1), \dots, s(\alpha_K)]$, where $s(\alpha_k) \in \mathcal{S}$ and \mathcal{S} is the M -ary constellation. Combining θ and \mathbf{s} , the MCIK-OFDM transmitted vector of the selected machine is generated as $\mathbf{x}_{q^*} = [x_{q^*}(1), \dots, x_{q^*}(N)]^T$, where $x_{q^*}(\alpha) = s(\alpha)$ for $\alpha \in \theta$ and $x_{q^*}(\alpha) = 0$ for $\alpha \notin \theta$. For each $\alpha \in \theta$, assume $\mathbb{E} \left\{ |x_{q^*}(\alpha)|^2 \right\} = \varphi E_s$, where E_s and φ are the average power per M -ary symbol and the power allocation coefficient, respectively.

For given N and K , there are $C(N, K)$ possible combinations of active sub-carrier indices, thus the number of index bits is given by $p_1 = \lfloor \log_2 C(N, K) \rfloor$. Meanwhile, the number of bits conveyed via K non-zero data symbols is $p_2 = K \log_2 M$. Consequently, the data rate of system can be given as

$$R = \frac{\lfloor \log_2 C(N, K) \rfloor + K \log_2 M}{N}. \quad (2)$$

At the AP, the received signal from the selected machine in the frequency domain, is given by

$$\mathbf{y}_{q^*} = \mathbf{H}_{q^*} \mathbf{x}_{q^*} + \mathbf{n}_{q^*}, \quad (3)$$

where $\mathbf{H}_{q^*} = \text{diag}[h_{q^*}(1), \dots, h_{q^*}(N)]$ is the channel matrix, and \mathbf{n}_{q^*} denotes the additive white Gaussian noise (AWGN) vector of machine q^* with its entries

satisfying $n_{q^*}(\alpha) \sim \mathcal{CN}(0, N_0)$. Denote by $\bar{\gamma}$ the average signal-to-noise ratio (SNR) per active sub-carrier, which is given as $\bar{\gamma} = \varphi E_s / N_0$.

For signal detection, the maximum likelihood (ML) is employed, carrying out an exhaustive search as follows

$$(\hat{\theta}, \hat{\mathbf{s}}) = \arg \min_{\theta, \mathbf{s}} \|\mathbf{y}_{q^*} - \mathbf{H}_{q^*} \mathbf{x}_{q^*}\|^2. \quad (4)$$

Then, $\hat{\theta}$ and $\hat{\mathbf{s}}$ are used to recover p transmitted data bits. Next, we analyze the SEP performance of the proposed OS-MCIK-OFDM with the ML detection.

3 SEP Performance Analysis

To derive the closed-form expression for the SEP of OS-MCIK-OFDM using the ML, it is essential to know distribution characteristics of the instantaneous SNRs of the selected machine. Thus, we introduce the following important theorem and its corollary.

Theorem 1. Denote $\gamma_{q,\alpha} = \bar{\gamma} |h_q(\alpha)|^2$ be the instantaneous SNR of the q -th machine at sub-carrier α . Based on (1), the selected machine satisfies $q^* = \arg \{\max_{q=1, \dots, Q} [\min_{\alpha=1, \dots, N} (\gamma_{q,\alpha})]\}$. Then, the moment generating function (MGF) of $\gamma_{q^*,\alpha}$ is approximated, at high SNRs, by

$$\mathcal{M}_{\gamma_{q^*,\alpha}}(t) \approx \frac{N^{Q-1} Q!}{\prod_{q=1}^Q (qN - t\bar{\gamma})}. \quad (5)$$

Proof. See Appendix A.

Notice that although we can not find out the exact MGF of $\gamma_{q^*,\alpha}$, its approximation in (5) is still capable of providing a tight closed-form expression for the SEP of OS-MCIK-OFDM.

Corollary 1. Denote $\gamma_{\Sigma_{q^*}} = \gamma_{q^*,\alpha} + \gamma_{q^*,\tilde{\alpha}}$, where $\gamma_{q^*,\alpha} = \bar{\gamma} |h_{q^*}(\alpha)|^2$ and $\alpha \neq \tilde{\alpha} = 1, \dots, N$, then the MGF of $\gamma_{\Sigma_{q^*}}$ can be approximated by

$$\mathcal{M}_{\gamma_{\Sigma_{q^*}}}(t) \approx \left[\frac{N^{Q-1} Q!}{\prod_{q=1}^Q (qN - t\bar{\gamma})} \right]^2. \quad (6)$$

Proof. Since $\gamma_{q^*,\alpha}$ and $\gamma_{q^*,\tilde{\alpha}}$ are the i.i.d RVs, we have $\mathcal{M}_{\gamma_{\Sigma_{q^*}}}(t) = \mathcal{M}_{\gamma_{q^*,\alpha}}^2(t)$, where $\mathcal{M}_{\gamma_{q^*,\alpha}}(t)$ is given in (5). This concludes the proof.

3.1 SEP Derivation

We first recall the definition of a symbol error event for MCIK-OFDM in [17] that a symbol error event occurs if any of the $K + 1$ symbols including K non-zero M -ary symbols and one index symbol θ are incorrectly decoded. As a result,

there are a maximum of $K + 1$ symbols in error events. Based on this definition, the average SEP of OS-MCIK-OFDM can be given by [17]

$$\bar{P}_s \leq \frac{\bar{P}_I \left(2 - \frac{1}{M}\right) + K\bar{P}_M}{K + 1}, \tag{7}$$

where \bar{P}_M denotes the average SEP of classical M -ary symbols and \bar{P}_I is the average index error probability (IEP). Notice that both \bar{P}_I and \bar{P}_M depend on the channel characteristics of the selected machine. Particularly, utilizing Theorem 1, \bar{P}_M of the q^* -th machine using M -ary PSK symbols can be obtained as in the following lemma.

Lemma 1. *The average SEP of classical M -ary symbols (PSK) of the selected machine q^* in (1) is approximated by*

$$\bar{P}_M \approx \frac{\xi\Psi}{12} \left[\frac{1}{\prod_{q=1}^Q (qN + \rho\bar{\gamma})} + \frac{3}{\prod_{q=1}^Q (qN + 4\rho\bar{\gamma}/3)} \right], \tag{8}$$

where $\xi = 1, 2$ for $M = 2$ and $M > 2$, respectively, $\Psi = N^{Q-1}Q!$ and $\rho = \sin^2(\pi/M)$.

Proof. See Appendix B.

The instantaneous IEP of machine q^* using the ML (denoted by P_I) can be approximated by [17]

$$P_I \approx \frac{K}{N} \sum_{\alpha=1}^N \sum_{\tilde{\alpha} \neq \alpha=1}^{N-K} Q \left(\sqrt{\frac{\gamma_{q^*,\alpha} + \gamma_{q^*,\tilde{\alpha}}}{2}} \right), \tag{9}$$

where $\gamma_{\Sigma_{q^*}} = \gamma_{q^*,\alpha} + \gamma_{q^*,\tilde{\alpha}}$. Applying the approximation of Q-function as $Q(x) \leq \frac{1}{2}e^{-\frac{x^2}{2}}$ to (9), we obtain

$$P_I \approx \frac{K}{2N} \sum_{\alpha=1}^N \sum_{\tilde{\alpha} \neq \alpha=1}^{N-K} e^{-\frac{\gamma_{q^*,\alpha} + \gamma_{q^*,\tilde{\alpha}}}{4}}. \tag{10}$$

Here, utilizing the MGF approach to (9) with the MGF of $\gamma_{\Sigma_{q^*}}$ given in Corollary 1, we attain

$$\bar{P}_I \approx \frac{K(N - K)}{2} \left[\frac{4^Q N^{Q-1} Q!}{\prod_{q=1}^Q (4qN + \bar{\gamma})} \right]^2. \tag{11}$$

Finally, plugging (8) and (11) into (7), the average SEP of the selected machine is obtained in the closed-form as

$$\begin{aligned} \bar{P}_s \approx & \frac{K(N - K) \left(2 - \frac{1}{M}\right)}{2(K + 1)} \left[\frac{4^Q N^{Q-1} Q!}{\prod_{q=1}^Q (4qN + \bar{\gamma})} \right]^2 \\ & + \frac{\xi K N^{Q-1} Q!}{12(K + 1)} \left[\frac{1}{\prod_{q=1}^Q (qN + \rho\bar{\gamma})} + \frac{3}{\prod_{q=1}^Q (qN + \frac{4\rho\bar{\gamma}}{3})} \right]. \end{aligned} \tag{12}$$

3.2 Asymptotic Analysis

We asymptotically investigate the SEP performance of OS-MCIK-OFDM to provide insights into achievable diversity and coding gains, as well as impacts of system parameters such as N , K and Q on the performance.

Specifically, at high SNRs, the average SEP in (12) can be asymptotically approximated by

$$\bar{P}_s \approx \frac{\xi K^{Q+1} Q! \left(1 + \frac{3^{Q+1}}{4^Q}\right)}{12N(K+1)\rho^Q} \left(\frac{1}{\gamma_0^Q}\right), \quad (13)$$

where $\gamma_0 = E_s/N_0$ is the average SNR per sub-carrier. This leads to the coding gain given by

$$c = \frac{\rho}{K} \sqrt[Q]{\frac{12N(K+1)}{\xi K Q! \left(1 + \frac{3^{Q+1}}{4^Q}\right)}}. \quad (14)$$

It is shown via (13) that OS-MCIK-OFDM achieves the diversity order of Q . Thus, a larger Q can significantly enhance the error performance of systems. However, increasing Q leads to a decrease in the coding gain, due to $\lim_{Q \rightarrow \infty} c = \lim_{Q \rightarrow \infty} \frac{\rho}{K} \sqrt[Q]{\frac{1}{Q!}} = 0$. Moreover, as can be seen from (14), the coding gain can be improved if K gets smaller or N gets larger, however at the cost of the spectral efficiency.

We now compare the proposed OS-MCIK-OFDM with the opportunistic scheduling OFDM (OS-OFDM) which is also based on the criterion (1). The average SEP of OS-OFDM (denoted by \bar{P}_{s_0}) can be attained from (13) when K tends to N , as follows

$$\bar{P}_{s_0} \approx \frac{\xi N^{Q-1} Q! \left(1 + \frac{3^{Q+1}}{4^Q}\right)}{12\rho^Q} \left(\frac{1}{\gamma_0^Q}\right). \quad (15)$$

Using (13) and (15), the coding gain achieved by OS-MCIK-OFDM over OS-OFDM is calculated by $g = 10 \log_{10} (\bar{P}_{s_0}/\bar{P}_s)^{1/Q}$, which is

$$g = 10 \log_{10} \left(\frac{N}{K} \sqrt[Q]{\frac{K+1}{K}}\right) \text{ (dB)}. \quad (16)$$

As seen from (16), increasing Q makes g smaller, however g always satisfies a lower bound that $g \geq 10 \log_{10} \left(\frac{N}{K}\right)$ for every Q . In addition, when $Q = 1$, (16) becomes [17, Eq. (27)], which validates the accuracy of our analysis.

4 Simulation Results

Simulation results are now presented to validate the performance of the proposed OS-MCIK-OFDM, the theoretical analysis as well as its superiority over OS-OFDM, under independent and identically distributed Rayleigh fading channels.

Figure 1 depicts the average SEP of OS-MCIK-OFDM when $(N, K, M) = (4, 1, 4)$ and $Q \in \{1, 2, 4, 6, 8\}$. Both the theoretical and asymptotic results are also provided. As observed from Fig. 1, the SEP performance of the proposed scheme is significantly improved when increasing Q . For example, when $Q = 2$ and at $\text{BER} = 10^{-4}$, our scheme achieves an SNR gain of 13 dB over MCIK-OFDM with $Q = 1$. Moreover, this gain increases to approximately 20 dB when $Q = 4$. However, if Q gets larger than 4, i.e., $Q = 6$ or 8, the performance gain attained becomes insignificant. This is caused by the decrease of the coding gain c when increasing Q as analyzed in Subsect. 3.2. In addition, Fig. 1 validates the tightness of derived theoretical and asymptotic expressions for the average SEP of OS-MCIK-OFDM, especially at higher SNRs.

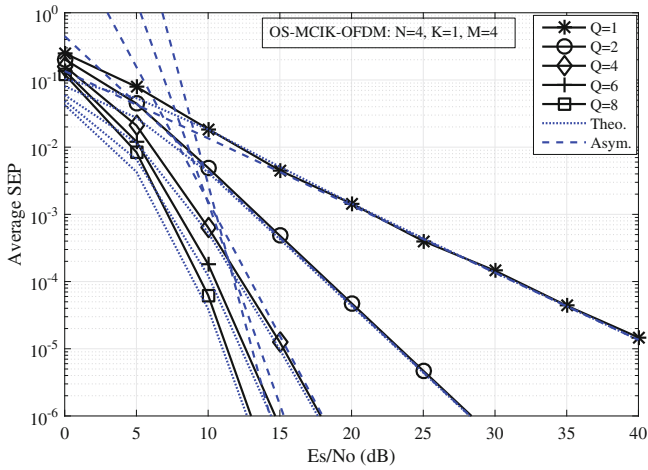


Fig. 1. SEP performance of OS-MCIK-OFDM when $(N, K, M) = (4, 1, 4)$ and $Q \in \{1, 2, 4, 6, 8\}$.

In Fig. 2, we compare the average SEPs between OS-MCIK-OFDM with $(N, K, M) = (2, 1, 2)$ and OS-OFDM with $(N, K) = (2, 2)$, at the same data rate of 1 bps/Hz and $Q \in \{1, 2, 4, 8\}$. It can be seen from Fig. 2 that our proposed scheme remarkably outperforms its benchmark, especially when Q is not too large. For instance, when $Q = 2$ and at high SNRs, the proposed scheme provides an SNR gain of more than 4 dB over OS-OFDM. This matches well with (16), which results in a similar gain of $g = 4.5$ dB. It also should be noted from Fig. 2 that when Q gets larger, the gap between two schemes becomes smaller, which confirms our analysis at the end of Subsect. 3.2.

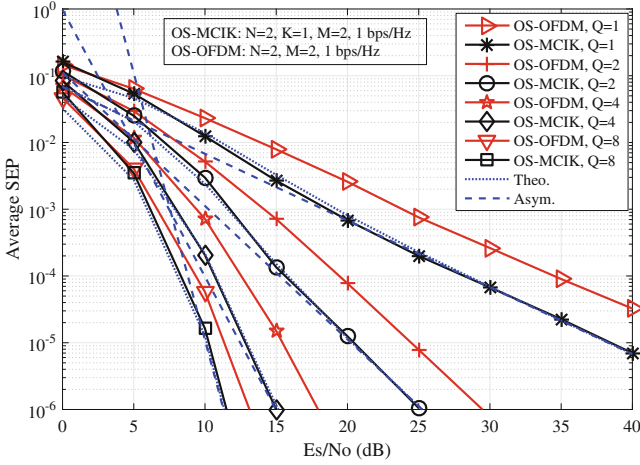


Fig. 2. SEP comparison between OS-MCIK-OFDM with $(N, K, M) = (2, 1, 2)$ and OS-OFDM with $(N, M) = (2, 2)$, when $Q \in \{1, 2, 4, 8\}$, at the same data rate of 1 bps/Hz.

5 Conclusions

We have proposed the opportunistic scheduling MCIK-OFDM (OS-MCIK-OFDM) and analyzed the SEP performance. In particular, the tight closed-form expression for the average SEP was derived. Then, the asymptotic analysis was conducted to provide insights into the SEP performance as well as impacts of system parameters such as N , K , and Q . More specifically, the proposed scheme achieves the diversity order being the number of machines, i.e., Q , and the achievable coding gain decreases when Q increases. Simulation results clearly validated the theoretical analysis, and particularly the superiority of the proposed scheme over the OS-OFDM, especially when Q is in a moderate size. In the future work, the proposed method can be extended to more realistic cases with non-identically distributed fading channels and imperfect CSI condition.

Appendix A

Proof of Theorem 1

Based on system model with the Rayleigh fading, it can be shown that $\gamma_{q,\alpha} = \bar{\gamma} |h_q(\alpha)|^2$ are the i.i.d RVs with the probability density function (PDF) and the cumulative distribution function (CDF), respectively, given by

$$f_\gamma(x) = \frac{1}{\bar{\gamma}} e^{-\frac{x}{\bar{\gamma}}}, \quad (17)$$

$$F_\gamma(x) = 1 - e^{-\frac{x}{\bar{\gamma}}}. \quad (18)$$

Relying on the scheduling method in (1), we first find the distribution of the following RV $\gamma_{q^*} = \max_{q=1,\dots,Q} [\min_{\alpha=1,\dots,N} (\gamma_{q,\alpha})]$. For this, denote $\gamma_q = \min_{\alpha=1,\dots,N} (\gamma_{q,\alpha})$ for given q . Using the order statistics, the CDF of γ_q can be calculated as

$$F_{\gamma_q}(x) = 1 - [1 - F_{\gamma}(x)]^N = 1 - e^{-\frac{Nx}{\gamma}}. \quad (19)$$

Thus, $\gamma_{q^*} = \max_{q=1,\dots,Q} (\gamma_q)$ has the CDF given by

$$F_{\gamma_{q^*}}(x) = [F_{\gamma_q}(x)]^Q = \left(1 - e^{-\frac{Nx}{\gamma}}\right)^Q. \quad (20)$$

Owing to the fact that $\gamma_{q^*} = \min_{\alpha=1,\dots,N} (\gamma_{q^*,\alpha})$, the CDF of $\gamma_{q^*,\alpha}$ can be obtained by the following equation

$$F_{\gamma_{q^*,\alpha}}(x) = 1 - [1 - F_{\gamma_{q^*}}(x)]^N. \quad (21)$$

Substituting (20) into (21), then solving this equation, we obtain

$$F_{\gamma_{q^*,\alpha}}(x) = 1 - \left[1 - \left(1 - e^{-\frac{Nx}{\gamma}}\right)^Q\right]^{\frac{1}{N}}. \quad (22)$$

Here, the PDF of $\gamma_{q^*,\alpha}$ can be attained by taking the derivative of $F_{\gamma_{q^*,\alpha}}(x)$ in (22) as

$$f_{\gamma_{q^*,\alpha}}(x) = \frac{Q}{\gamma} \left[1 - \left(1 - e^{-\frac{Nx}{\gamma}}\right)^Q\right]^{\frac{1-N}{N}} \left(1 - e^{-\frac{Nx}{\gamma}}\right)^{Q-1} e^{-\frac{Nx}{\gamma}}. \quad (23)$$

As can be shown from (23), it is difficult to directly compute the MGF of $\gamma_{q^*,\alpha}$ based on its PDF in (23). Hence, this motivates us to find out an approximation of $f_{\gamma_{q^*,\alpha}}(x)$, that can facilitate the derivation of the MGF of $\gamma_{q^*,\alpha}$. For this, we consider (23) at high SNRs and discover that

$$\lim_{\bar{\gamma} \rightarrow \infty} \left[1 - \left(1 - e^{-\frac{Nx}{\gamma}}\right)^Q\right]^{\frac{1-N}{N}} = 1. \quad (24)$$

Consequently, the PDF of $\gamma_{q^*,\alpha}$ can be approximated, in high SNR regions, by

$$f_{\gamma_{q^*,\alpha}}(x) \approx \frac{Q}{\gamma} \left(1 - e^{-\frac{Nx}{\gamma}}\right)^{Q-1} e^{-\frac{Nx}{\gamma}}. \quad (25)$$

Finally, the MGF of $\gamma_{q^*,\alpha}$ can be calculated, by performing the inverse Laplace transform in (25), as follows

$$\begin{aligned}
 \mathcal{M}_{\gamma_{q^*,\alpha}}(z) &\approx \mathcal{L}^{-1} \left\{ \frac{Q}{\bar{\gamma}} \left(1 - e^{-\frac{Nx}{\bar{\gamma}}} \right)^{Q-1} e^{-\frac{Nx}{\bar{\gamma}}} \right\} \\
 &= \mathcal{L}^{-1} \left\{ \frac{Q}{\bar{\gamma}} \sum_{q=0}^{Q-1} C(Q-1, q) (-1)^q e^{-\frac{(q+1)Nx}{\bar{\gamma}}} \right\} \\
 &= Q \sum_{q=0}^{Q-1} \frac{C(Q-1, q) (-1)^q}{(q+1)N - t\bar{\gamma}} \\
 &= \frac{N^{Q-1} Q!}{\prod_{q=1}^Q (qN - t\bar{\gamma})}. \tag{26}
 \end{aligned}$$

The theorem is completely proved.

Appendix B

Proof of Lemma 1

According to [20], the instantaneous SEP of M -ary PSK symbols can be approximated by $P_M(\alpha) \approx \xi Q(\sqrt{2\gamma_{q^*,\alpha}} \sin(\pi/M))$, where we recall $\gamma_{q^*,\alpha}$ being the instantaneous SNR of the selected machine at sub-carrier α , and $\xi = 1$ for $M = 2$ and $\xi > 1$ for $M > 2$. Using the approximation of Q -function as $Q(x) \approx \frac{1}{12}e^{-\frac{x^2}{2}} + \frac{1}{4}e^{-\frac{2x^2}{3}}$, we obtain

$$P_M(\alpha) \approx \frac{\xi}{12} \left(e^{-\gamma_{q^*,\alpha}\rho} + 3e^{-\frac{4\gamma_{q^*,\alpha}\rho}{3}} \right), \tag{27}$$

where $\rho = \sin^2(\pi/M)$.

Next, applying the MGF approach in (27), with the MGF of $\gamma_{q^*,\alpha}$ given in Theorem 1, the average SEP of the classical M -ary PSK symbols of machine q^* can be computed as

$$\begin{aligned}
 \bar{P}_M &\approx \mathbb{E}_{\gamma_{q^*,\alpha}} \left\{ \frac{\xi}{12} \left(e^{-\gamma_{q^*,\alpha}\rho} + 3e^{-\frac{4\gamma_{q^*,\alpha}\rho}{3}} \right) \right\} \\
 &= \frac{\xi}{12} [\mathcal{M}_{\gamma_{q^*,\alpha}}(\rho) + \mathcal{M}_{\gamma_{q^*,\alpha}}(-4\rho/3)] \\
 &= \frac{\xi N^{Q-1} Q!}{12} \left[\frac{1}{\prod_{q=1}^Q (qN + \rho\bar{\gamma})} + \frac{3}{\prod_{q=1}^Q (qN + \frac{4\rho\bar{\gamma}}{3})} \right].
 \end{aligned}$$

This concludes the proof.

References

1. Abu-alhiga, R., Haas, H.: Subcarrier-index modulation OFDM. In: Proceedings of IEEE International Symposium on Personal, Indoor and Mobile Radio Communications, pp. 177–181, September 2009

2. Basar, E., Aygolu, U., Panayirci, E., Poor, H.V.: Orthogonal frequency division multiplexing with index modulation. *IEEE Trans. Signal Process.* **61**(22), 5536–5549 (2013)
3. Basar, E., Wen, M., Mesleh, R., Renzo, M.D., Xiao, Y., Haas, H.: Index modulation techniques for next-generation wireless networks. *IEEE Access* **5**, 16693–16746 (2017)
4. Luong, T.V., Ko, Y., Choi, J.: Repeated MCIK-OFDM with enhanced transmit diversity under CSI uncertainty. *IEEE Trans. Wireless Commun.* **17**(6), 4079–4088 (2018)
5. Luong, T.V., Ko, Y.: A closed-form symbol error probability for MCIK-OFDM with frequency diversity. In: *Proceedings of IEEE SPAWC*, July 2017, pp. 1–5 (2017)
6. Basar, E.: OFDM with index modulation using coordinate interleaving. *IEEE Wireless Commun. Lett.* **4**(4), 381–384 (2015)
7. Zheng, J., Chen, R.: Achieving transmit diversity in OFDM-IM by utilizing multiple signal constellations. *IEEE Access* **5**(99), 8978–8988 (2017)
8. Ko, Y.: A tight upper bound on bit error rate of joint OFDM and multi-carrier index keying. *IEEE Commun. Lett.* **18**(10), 1763–1766 (2014)
9. Wen, M., Cheng, X., Ma, M., Jiao, B., Poor, H.V.: On the achievable rate of OFDM with index modulation. *IEEE Trans. Signal Process.* **64**(8), 1919–1932 (2016)
10. Luong, T.V., Ko, Y.: Symbol error outage performance analysis of MCIK-OFDM over complex TWDP fading. In: *Proceedings of European Wireless*, May 2017, pp. 1–5 (2017)
11. Crawford, J., Chatziantoniou, E., Ko, Y.: On the SEP analysis of OFDM index modulation with hybrid low complexity greedy detection and diversity reception. *IEEE Trans. Veh. Technol.* **66**(9), 8103–8118 (2017)
12. Luong, T.V., Ko, Y.: The BER analysis of MRC-aided greedy detection for OFDM-IM in presence of uncertain CSI. *IEEE Wireless Commun. Lett.*, to be published
13. Zheng, B., Chen, F., Wen, M., Ji, F., Yu, H., Liu, Y.: Low-complexity ML detector and performance analysis for OFDM with in-phase/quadrature index modulation. *IEEE Commun. Lett.* **19**(11), 1893–1896 (2015)
14. Mao, T., Wang, Z., Wang, Q., Chen, S., Hanzo, L.: Dual-mode index modulation aided OFDM. *IEEE Access* **5**, 50–60 (2017)
15. Wen, M., Basar, E., Li, Q., Zheng, B., Zhang, M.: Multiple-mode orthogonal frequency division multiplexing with index modulation. *IEEE Trans. Commun.* **65**(9), 3892–3906 (2017)
16. Basar, E.: On multiple-input multiple-output OFDM with index modulation for next generation wireless networks. *IEEE Trans. Signal Process.* **64**(15), 3868–3878 (2016)
17. Luong, T.V., Ko, Y.: Impact of CSI uncertainty on MCIK-OFDM: tight, closed-form symbol error probability analysis. *IEEE Trans. Veh. Technol.* **67**(2), 1272–1279 (2018)
18. Van Luong, T., Ko, Y.: A tight bound on BER of MCIK-OFDM with greedy detection and imperfect CSI. *IEEE Commun. Lett.* **21**(12), 2594–2597 (2017)
19. Luong, T.V., Ko, Y., Choi, J.: Precoding for spread OFDM IM. In: *Proceedings of IEEE 87th Vehicular Technology Conference (VTC Spring)*, pp. 1–5 (2018)
20. Proakis, J.: *Digital Communications*. McGraw-Hill, New York City (2001)